ELSEVIER

Journal of Fluorine Chemistry 112 (2001) 233–240

JOURNAL OF FLUORINE CHEMISTRY

www.elsevier.com/locate/jfluchem

Electrochemical characteristics and structures of surface-fluorinated graphites with different particle sizes for lithium ion secondary batteries

Vinay Gupta[a], Tsuyoshi Nakajima[a,*], Yoshimi Ohzawa[a], Hiroyuki Iwata[b]

[a]*Department of Applied Chemistry, Aichi Institute of Technology, Yakusa-cho, Toyota-shi 470-0392, Japan*
[b]*Technical Research Center, Aichi Institute of Technology, Yakusa-cho, Toyota-shi 470-0392, Japan*

Received 29 May 2001; accepted 31 August 2001

Dedicated to Dr. Karl O. Christe for his 65th birthday

Abstract

Electrochemical characteristics of surface-fluorinated graphite samples with average particle diameters of 25 and 40 μm (NG-25 and NG-40) have been investigated in 1 mol dm^{-3} $LiClO_4$–ethylene carbonate (EC)/diethyl carbonate (DEC) at 25 °C. The fluorine contents obtained by elemental analysis are 0.2–0.4 at.% and the surface fluorine concentrations obtained by X-ray photoelectron spectroscopy (XPS) are 4–12 at.% for the samples fluorinated between 150 and 300 °C. Raman spectra and transmission electron micrographs indicate the increase in the surface disordering of graphite. The surface areas of graphite samples are increased by 64–77% and the mesopores with diameter of 2–3 nm are also increased by surface fluorination. The charge capacities of surface-fluorinated samples are larger than those of original graphites and even the theoretical capacity of graphite, 372 mAh g^{-1}. The increments of the capacities are ~10 and ~13% for 25 and 40 μm graphite samples, respectively. Nevertheless, the first Coulombic efficiencies are the same as those of original graphites for the samples fluorinated between 150 and 300 °C. The increase in the capacities was discussed on the basis of surface compositions and structures of fluorinated graphite samples. © 2001 Elsevier Science B.V. All rights reserved.

Keywords: Surface modification; Surface fluorination; Graphite electrode; Lithium ion battery

1. Introduction

Lithium ion secondary batteries are currently used for portable telephones, personal computers, cameras and so on. It is also expected that they are used for energy storage and electric vehicles in near future. Lithium ion batteries consist of oxide cathode such as $LiCoO_2$, carbonaceous anode and organic solvents containing $LiPF_6$. Carbon materials such as synthetic and natural graphites, carbon and graphite fibers, non-graphitizing carbons and so on are now employed as anode materials. Crystallinity, surface area, surface pore volume distribution and nature of surface chemical species are important factors influencing the electrochemical properties of carbonaceous electrodes. Surface modification is one of the effective methods for improving the electrochemical characteristics of carbonaceous electrodes [1–9]. Several structural parameters such as surface area, surface pore volume distribution and surface chemical species would influence the reaction kinetics because the electrochemical intercalation and deintercalation of lithium ions occur at the edge plane and through surface crack of carbon materials. In order to improve the characteristics of carbonaceous electrodes, some methods of surface modification were applied. They are surface oxidation [1–3], surface fluorination [4–6], high temperature treatment under vacuum [7], metal coating [8] and carbon coating [9]. Light oxidation of graphite and carbon increases their capacities because of the formation of nanopores or nanochannels. However, strong oxidation causes the degradation of carbon materials, giving rise to an increase in the irreversible capacities [1,3]. Surface oxidation of mesocarbon microbeads is effective for improving the electrode kinetics due to the removal of its surface skin [2]. Heating of carbon fibers to ~1000 °C under vacuum effectively removes the surface oxygen species, leading to an increase in the reaction kinetics and capacities [7]. Thin metal coating is a method to activate the surface of carbon materials, increasing the reaction rates [8]. Carbon coating on graphite reduces the

* Corresponding author: Tel.: +81-565-48-8121x2201; fax: +81-565-48-0076.
E-mail address: nakajima@ac.aitech.ac.jp (T. Nakajima).

0022-1139/01/$ – see front matter © 2001 Elsevier Science B.V. All rights reserved.
PII: S0022-1139(01)00517-6

irreversible capacities and increases the Coulombic efficiencies [9]. Surface fluorination by elemental fluorine and plasma fluorination using CF_4 increase the capacities to the values higher than those of original graphites and the theoretical capacity of graphite, 372 mAh g^{-1}, corresponding to the fully lithium-intercalated graphite, LiC_6 [5,6]. Surface area is decreased with increasing particle size of graphite powder. Average particle size of graphite is one of the important factors influencing the electrode characteristics because the capacity usually decreases with increasing particle size of graphite. It is, therefore, expected that the effect of surface modification is more clearly observed for graphite samples having the larger particle sizes. In this study, we have investigated the electrochemical characteristics of surface-fluorinated graphite samples with average particle diameters of 25 and 40 μm in comparison with the results previously obtained for surface-fluorinated graphite samples with average particle size of 7 μm [5] and discussed about the relation between the electrochemical properties and surface structures of surface-fluorinated graphite samples.

2. Experimental

2.1. Surface fluorination of graphite powder

Starting materials are natural graphite powder with average particle diameters of 25 and 40 μm (NG-25 and NG-40) supplied by Japan Storage Battery Co. Ltd. and fluorine gas (purity: 99.4–99.7%) supplied by Daikin Industries Ltd. Surface fluorination of graphite powder (≈170 mg) was made at 150–500 °C by elemental fluorine of 3×10^4 Pa for 2 min in a nickel reactor. For the measurements of surface area and pore volume distribution, natural graphite powder with average particle diameter of 7 μm (NG-7) was also fluorinated at 150, 250 and 350 °C by elemental fluorine of 3×10^4 Pa for 2 min.

2.2. Analyses of the surface-fluorinated graphite samples

The compositions of surface-fluorinated graphite samples were determined by elemental analysis of carbon and fluorine at Faculty of Pharmaceutical Science, Elemental Analysis Center, Kyoto University. The amount of oxygen was calculated by subtracting the analytical values for carbon and fluorine from 100%. Surface compositions were determined from the peak areas of C 1s, F 1s and O 1s spectra obtained by X-ray photoelectron spectroscopy (XPS, Ulvac Phi Model 5500 with Mg Kα radiation). The nature of C–F bonding was also evaluated by XPS. The binding energies of photoelectron peaks were determined relative to that of C 1s electron of graphite (284.3 eV) without charging correction. The surface disordering of graphite was examined by Raman spectroscopy (Jobin-Yvon, T-64000 with Ar ion laser of 514.5 nm). The peak intensity ratios in Raman shifts observed at 1360 and 1580 cm^{-1} were calculated as R values (I_D/I_G) to evaluate the degree of surface disordering. Surface areas and pore volume distribution of surface-fluorinated graphite samples were measured by BET method using nitrogen gas (Micromeritics, Gemini 2375).

2.3. Electrochemical measurement

The galvanostatic charge/discharge cycling for surface-fluorinated graphite samples was performed at 25 °C using three electrodes glass cell in a glove box filled with argon. The preparative method of graphite electrode was described in a previous paper [5]. The graphite electrode was prepared so that the amount of the binder (polyvinylidene fluoride (PVDF)) was 20 wt.%. The counter and reference electrodes were metallic lithium pressed onto nickel mesh, and electrolyte solution was 1 mol dm^{-3} $LiClO_4$–ethylene carbonate (EC)/diethyl carbonate (DEC) (1:1 in volume). The charge/discharge cycling was performed at a current density of 60 mA g^{-1} between 0 and 3 V versus Li/Li^+. The current densities per unit surface area can be calculated using the data of surface areas given in Table 3. They are (16–9.9) $\times 10^{-4}$ and (20–12) $\times 10^{-4}$ mA cm^{-2} for NG-25 and NG-40, respectively.

3. Results and discussion

3.1. Surface compositions and structure of fluorinated graphite samples

When graphite is allowed to react with elemental fluorine, fluorine is intercalated in graphite, yielding fluorine–graphite intercalation compounds with ionic or semi-ionic C–F bond below ca. 100 °C, and graphite fluoride with covalent C–F bond between ca. 350 and 600 °C [10,11]. However, only surface of graphite is fluorinated between ca. 100 and 350 °C. Fluorine contents obtained by elemental analysis are less than 1 at.% for 25 μm graphite samples (NG-25) fluorinated between 150 and 350 °C and for 40 μm graphite samples (NG-40) fluorinated between 150 and 300 °C as given in Table 1. With increasing fluorination temperature, the fluorine contents are also increased, being between 1.2 and 4.7 at.% for 25 μm graphites and between 1.7 and 4.2 at.% for 40 μm samples. The surface fluorine concentrations obtained by XPS have the similar trend, that is, are less than 10 at.% for 25 μm graphites fluorinated between 150 and 350 °C and for 40 μm graphites fluorinated between 150 and 250 °C. The surface fluorine concentrations are also increased with increasing fluorination temperature. The total fluorine contents should be less than about 1 at.% because fluorine reacts with lithium in the reduction process to give LiF and decreases the first Coulombic efficiency [5,6]. A small amount of fluorine less than 1 at.% does not give a negative effect to the electrode characteristics [5,6].

Table 1
Compositions of surface-fluorinated graphite samples, obtained by elemental analysis and calculated from the peak areas of XPS

Fluorination temperature (°C)	Elemental analysis (at.%)			XPS (at.%)		
	C	F	O	C	F	O
150[a]	99.4	0.3	0.3	92.2	4.5	3.3
200[a]	99.0	0.3	0.7	90.7	5.6	3.7
250[a]	99.5	0.4	0.1	90.7	6.1	3.2
300[a]	99.6	0.4	0.0	90.1	6.9	3.0
350[a]	99.4	0.6	0.0	89.6	8.1	2.3
400[a]	98.8	1.2	0.0	84.6	13.1	2.3
450[a]	95.9	3.7	0.3	79.3	19.1	1.6
500[a]	95.0	4.7	0.3	69.6	28.9	1.5
150[b]	99.8	0.2	0.0	95.2	3.6	1.2
200[b]	99.8	0.2	0.0	93.3	5.6	1.1
250[b]	99.7	0.3	0.0	90.8	8.2	1.0
300[b]	99.6	0.4	0.0	86.2	12.0	1.8
350[b]	98.3	1.7	0.0	83.8	14.3	1.9
400[b]	97.1	2.9	0.0	77.1	20.9	2.0
450[b]	95.4	4.1	0.5	71.1	26.0	2.9
500[b]	95.3	4.2	0.5	65.4	33.1	1.5

[a] NG-25: natural graphite powder with average particle diameter of 25 μm.
[b] NG-40: natural graphite powder with average particle diameter of 40 μm.

X-ray photoelectron spectra also indicate the nature of C–F bonding. Typical spectra are shown in Fig. 1 and the results are summarized in Table 2. F 1s spectra have single peak located at 687.7 ± 0.2 and 687.8 ± 0.2 eV, and the corresponding C 1s peaks are observed at 288.9 ± 0.2 and 288.7 ± 0.3 eV for 25 and 40 μm graphite samples, respectively. These binding energies correspond to the tertiary carbon atoms bonded to fluorine, and maybe a small amount of carboxyl groups. The binding energies show that the C–F bonds are intermediate between the semi-ionic and covalent bonds [5,6,10–14]. The shoulder peaks in C 1s spectra observed at 285.4 ± 0.3 and 285.0 ± 0.2 eV are due to carbon atoms neighboring to those bonded to fluorine and a small amount of carbon atoms bonded to hydroxyl and carbonyl groups. The very weak C 1s peaks at 291.0 ± 0.2 and 291.0 ± 0.3 eV show a plasmon satellite and a trace of covalently bonded fluorine. Weak O 1s peaks are also

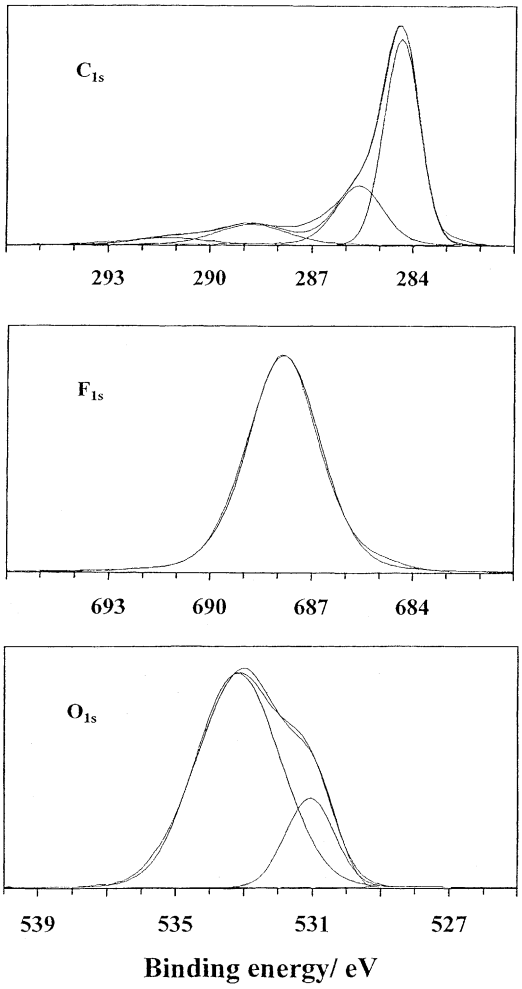

Fig. 1. X-ray photoelectron spectra of surface-fluorinated graphite sample. Graphite: NG-25 (≈25 μm), fluorination temperature: 250 °C.

observed at 531.0 ± 0.3, 532.8 ± 0.3 and 535.0 ± 0.3 eV, and 531.0 ± 0.6, 532.7 ± 0.6 and 534.8 ± 0.4 eV for 25 and 40 μm graphites, respectively. Among them, the first two peaks are due to carbonyl and hydroxyl groups, and the last ones are due to adsorbed water molecules.

Raman spectroscopy reveals the degree of surface disordering of carbon materials [15,16]. Fig. 2 shows the

Table 2
Binding energies of X-ray photoelectron spectra of surface-fluorinated graphite samples[a]

Original sample	C 1s (eV)	F 1s (eV)	O 1s (eV)
NG-25	284.25 ± 0.05 (40.8–65.3)	687.7 ± 0.2 (100)	531.0 ± 0.3 (19.2–32.9)
	285.4 ± 0.3 (19.3–30.3)		532.8 ± 0.3 (61.0–80.8)
	288.9 ± 0.2 (10.7–28.6)		535.0 ± 0.3 (6.1–6.8)
	291.0 ± 0.2 (3.4–5.1)		
NG-40	284.25 ± 0.05 (29.4–63.5)	687.8 ± 0.2 (100)	531.0 ± 0.6 (19.2–42.3)
	285.0 ± 0.2 (22.1–31.6)		532.7 ± 0.6 (57.7–74.0)
	288.7 ± 0.3 (9.6–42.1)		534.8 ± 0.4 (5.2–7.6)
	291.0 ± 0.3 (3.2–7.6)		

[a] Values shown in the parenthesis are in percent.

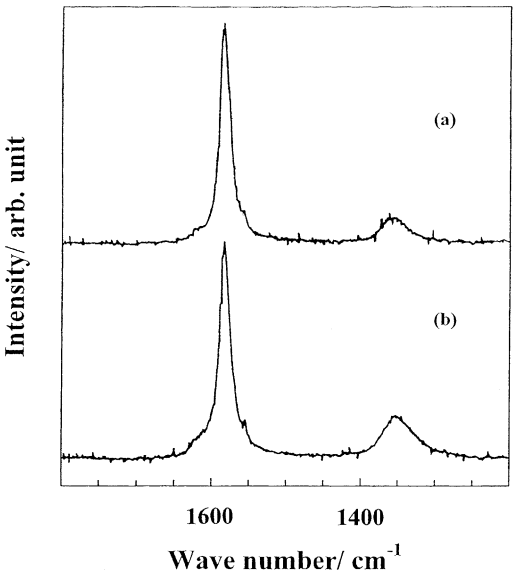

Fig. 2. Raman spectra of original graphite (a) and surface-fluorinated (b) sample. Graphite: NG-25 (≈25 μm), fluorination temperature: 250 °C.

typical Raman spectra of original graphite and surface-fluorinated sample. Graphite powder usually exhibits two Raman shifts at 1580 and 1360 cm^{-1}. The peak observed at 1580 cm^{-1} indicates E_{2g2} vibration mode derived from graphitic structure of carbon materials (G-band) and the other peak at 1360 cm^{-1} indicates A_{1g} mode arising from the disordered structure and/or edge of carbon particles (D-band) [15,16]. As shown in Fig. 2, graphite powder with high crystallinity has a strong peak at 1580 cm^{-1} and a weak one at 1360 cm^{-1}. The peak at 1360 cm^{-1} is slightly enhanced by surface fluorination, which means that the surface disordering of graphite powder is somewhat increased. Thus, the intensity ratio of two peaks, R (I_D/I_G), shows the degree of surface disordering of graphite powder. The results are given in Table 3. The R values of original graphite samples are 0.082 and 0.080 for 25 and 40 μm graphites, respectively. However, light fluorination increases the R values, that is, induces the surface disordering of graphite. The R values are increased with increase in the fluorination temperature, in particular, above 350 °C.

Table 3
R (I_D/I_G) values of Raman spectra of surface-fluorinated graphite samples

Graphite sample	R (NG-25)	R (NG-40)
Original graphite	0.082	0.080
Fluorinated at 150 °C	0.15	0.13
Fluorinated at 200 °C	–	0.14
Fluorinated at 250 °C	0.19	0.16
Fluorinated at 300 °C	0.18	0.23
Fluorinated at 350 °C	–	0.45
Fluorinated at 400 °C	0.40	0.74
Fluorinated at 450 °C	0.70	0.55
Fluorinated at 500 °C	0.56	0.73

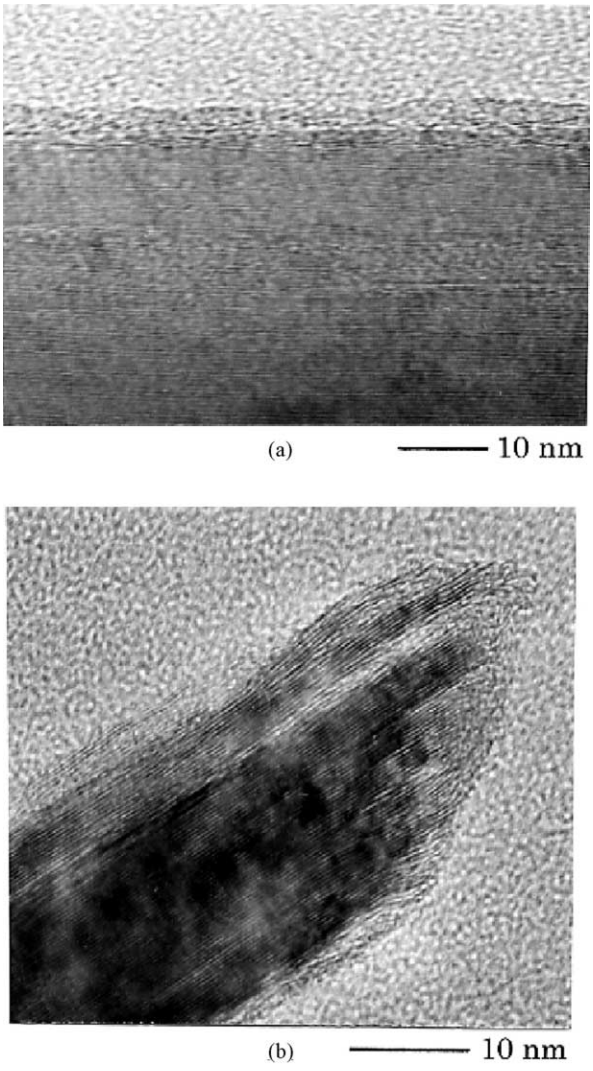

Fig. 3. Transmission electron microscopic images of surface-fluorinated graphite samples: (a) NG-25 (≈25 μm) fluorinated at 250 °C, (b) NG-40 (≈40 μm) fluorinated at 300 °C.

Fig. 3 shows transmission electron micrographs of surface-fluorinated graphite samples. Fig. 3(a) and (b) indicate fluorinated layers of basal and edge planes of graphite, respectively. The fluorinated surface layers have disordered morphology in contrast with the unreacted graphene layers. The thickness of the fluorinated basal plane is about 3–4 nm which corresponds to that of 5–7 fluorine intercalated layers since the thickness of a fluorine-intercalated layer is about 0.55 nm [10,11]. The fluorinated edge plane is also disordered with the similar thickness. The observed images coincide with the R values calculated from the peak areas of Raman spectra.

The results obtained by Raman spectroscopy and transmission electron microscopy suggest the change of surface area and pore volume distribution of graphite powder. Table 4 shows the surface areas of 7, 25 and 40 μm graphites (NG-7, NG-25 and NG-40) and surface-fluorinated samples, obtained by BET method. The surface areas of original

Table 4
Surface areas of graphite samples (≈7, 25 and 40 μm) and the samples fluorinated at 150, 250 and 350°C

Graphite sample	Surface area ($m^2\ g^{-1}$)		
	NG-7	NG-25	NG-40
Original graphite	4.79	3.71	2.94
Fluorinated at 150 °C	5.61	5.16	3.50
Fluorinated at 250 °C	7.65	5.18	4.90
Fluorinated at 350 °C	8.48	6.09	4.95

graphite samples are decreased with increase in their average particle sizes from 4.79 to 2.94 $m^2\ g^{-1}$. Table 4 indicates that fluorination effectively enlarges the surface area of graphite powder. The surface areas are increased with increasing fluorination temperature for all the graphite samples. The increments of the surface areas are in the range of 64–77%. Pore volume distribution data for the same samples are shown in Figs. 4–6. Original graphite samples have the mesopores with diameters of 1.5–2 to 8–10 nm in a wide range. Fluorination of graphite reduces the mesopores with the larger diameters. This trend becomes distinct with increase in the fluorination temperature for all the graphite samples. In any case, the mesopores with diameter of 2–3 nm are significantly increased with increase in the fluorination temperature, and their rates finally reached 64, 60 and 57% for 7, 25 and 40 μm graphite samples, respectively. The enlargement of surface area and change in the pore volume distribution would be induced by carbon–carbon bond breaking by fluorination at high temperatures.

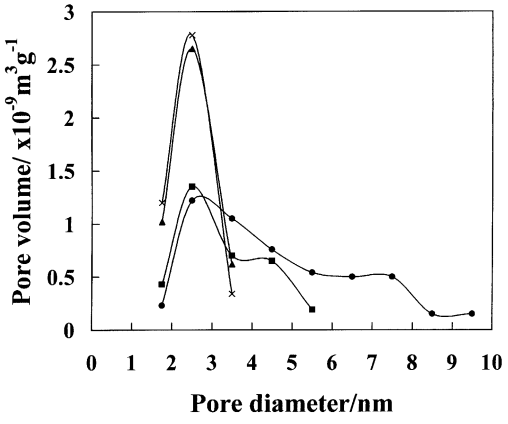

Fig. 4. Pore volume distribution of original and surface-fluorinated graphite samples: (●) NG-7 (≈7 μm), (■) fluorinated at 150 °C, (▲) fluorinated at 250 °C, (×) fluorinated at 350 °C.

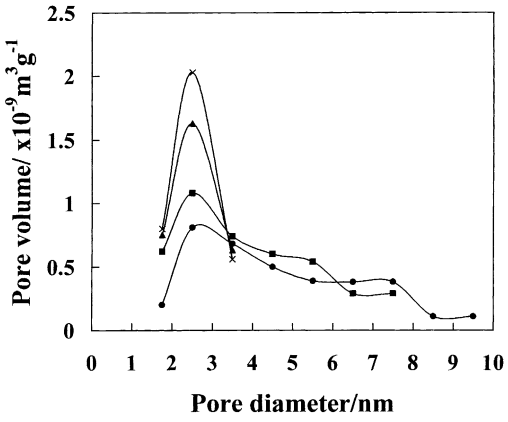

Fig. 5. Pore volume distribution of original and surface-fluorinated graphite samples: (●) NG-25 (≈25 μm), (■) fluorinated at 150 °C, (▲) fluorinated at 250 °C, (×) fluorinated at 350 °C.

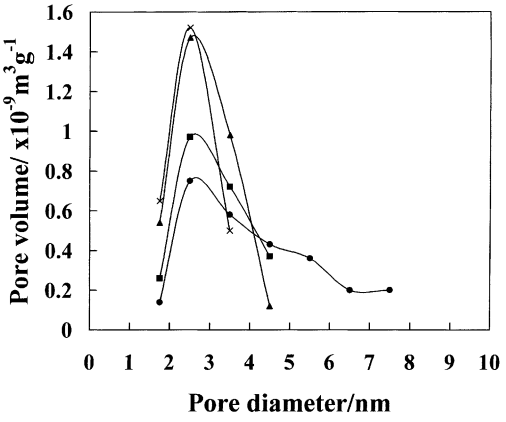

Fig. 6. Pore volume distribution of original and surface-fluorinated graphite samples: (●) NG-40 (≈40 μm), (■) fluorinated at 150 °C, (▲) fluorinated at 250 °C, (×) fluorinated at 350 °C.

3.2. Electrochemical properties of surface-fluorinated graphite samples with different particle sizes

The charge/discharge curves for original graphite (NG-25, ≈25 μm) and the same graphite fluorinated at 250 °C are shown in Fig. 7. The profile of the charge/discharge curves for other original and surface-fluorinated samples is the same as that shown in Fig. 7. A small potential plateau is observed at 0.6–0.7 V versus Li/Li^+ in the first reduction curve, being ascribed to the reduction of EC and subsequent formation of a thin surface film on graphite (solid electrolyte interphase (SEI)) [17]. The SEI enables the desolvation of lithium ions and its intercalation into graphene layers without degradation of graphitic structure. The potential plateau indicating the decomposition of EC is no longer observed from the 2nd cycle in any case. The surface-fluorinated graphite clearly shows the higher capacity than original graphite without any change in the profile of the charge/discharge curves. In addition, the capacities somewhat increase after 1st cycle in both original and surface-fluorinated samples as shown in Fig. 7.

The charge capacities for 25 μm graphite and surface-fluorinated samples are shown in Fig. 8 as a function of cycle number. The capacity of original 25 μm graphite is initially 350 mAh g^{-1} and gradually increases with cycling, reaching 353 mAh g^{-1} at 10th cycle. This value is somewhat lower than 363 mAh g^{-1} for 7 μm graphite previously studied

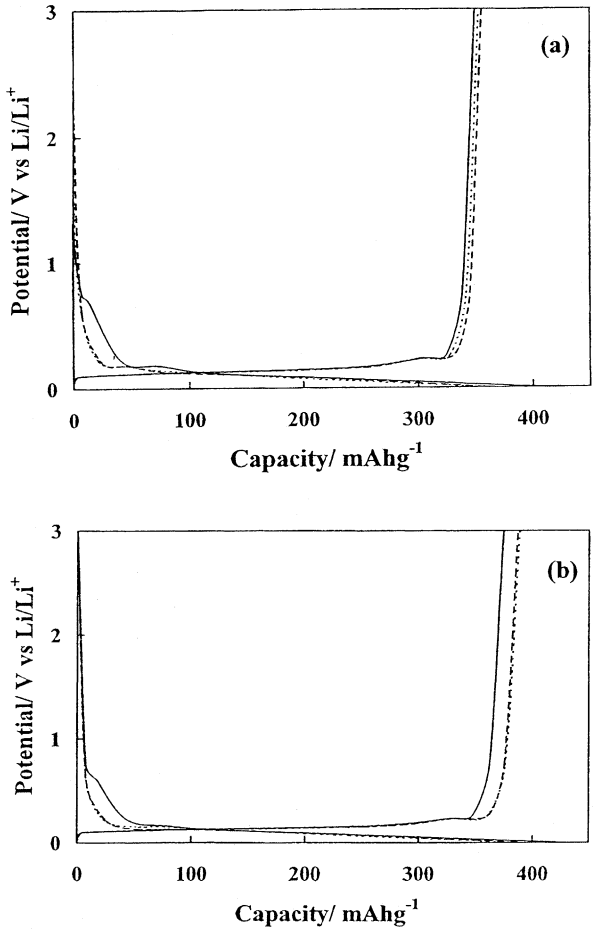

Fig. 7. Charge/discharge curves for original (a) and surface-fluorinated (b) graphite samples. Graphite: NG-25 (≈25 μm), fluorination temperature: 250 °C; (—) 1st cycle (···) 5th cycle (- - -) 10th cycle.

because 25 μm graphite has a smaller surface area than 7 μm graphite as given in Table 4 [5]. However, all surface-fluorinated graphite samples exhibit higher capacities than original graphite. Their capacities at 10th cycle are even higher than the theoretical value of graphite, 372 mAh g^{-1} except those of the samples fluorinated at 450 and 500 °C. Among the samples fluorinated between 150 and 400 °C, those fluorinated between 200 and 300 °C give the highest capacities of 387–389 mAh g^{-1}, and those fluorinated at 150 and 350 °C also show 382–384 mAh g^{-1} which are higher than 378 mAh g^{-1} for the sample fluorinated at 400 °C. The increments of the charge capacities obtained at 10th cycle are ∼10%, which is larger than ∼5% for surface-fluorinated graphite samples with average diameter of 7 μm [5]. The results are similar in case of 40 μm graphite as shown in Fig. 8. The capacity of original graphite is 335 mAh g^{-1} lower than that of 25 μm graphite at 10th cycle because of the smaller surface area of 40 μm graphite. The surface-fluorinated graphite samples, however, have the higher capacities than original graphite. The samples fluorinated between 150 and 300 °C exhibit the capacities of 374–377 mAh g^{-1} much higher than that for original graphite

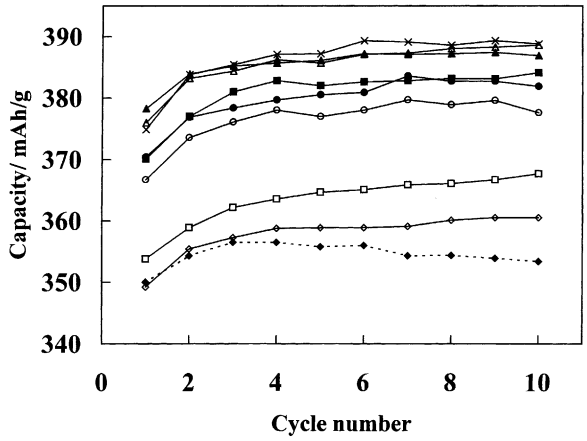

Fig. 8. Charge capacities of original and surface-fluorinated graphite samples as a function of cycle number: (◆) NG-25 (≈25 μm), (■) 150 °C, (▲) 200 °C, (×) 250 °C, (△) 300 °C, (●) 350 °C, (○) 400 °C, (□) 450 °C, (◇) 500 °C.

and even slightly higher than the theoretical value of graphite at 10th cycle. The capacities are gradually decreased with increase in the fluorination temperature; 368 mAh g^{-1} for the sample fluorinated at 350 °C, 361 mAh g^{-1} for those fluorinated at 400 and 450 °C, and 354 mAh g^{-1} for that fluorinated at 500 °C. The increments of the charge capacities are ∼13% at 10th cycle, which is also larger than ∼5% obtained for surface-fluorinated graphite samples with average particle diameter of 7 μm. In addition, the cycle ability is good for both kinds of surface-fluorinated samples with average particle diameters of 25 and 40 μm as shown in Figs. 8 and 9.

The capacities are increased with increase in the cycle not only in the surface-fluorinated graphites, but also even in the untreated samples and gradually stabilized after several cycles. The following reasons should be pointed out for the capacity increase with cycle. One is that the surface disordering of graphite is increased by electrochemical

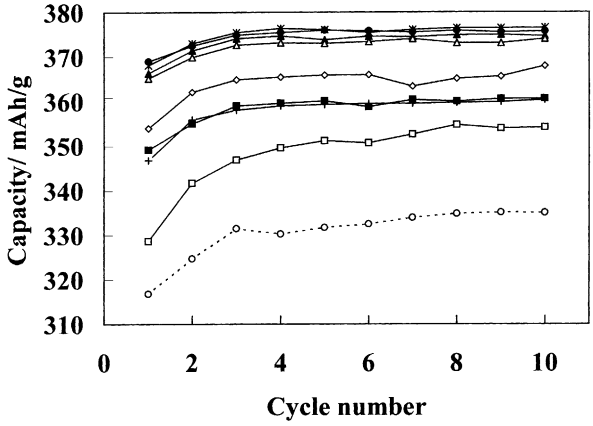

Fig. 9. Charge capacities of original and surface-fluorinated graphite samples as a function of cycle number: (○) NG-40 (≈40 μm), (▲) 150 °C, (△) 200 °C, (●) 250 °C, (×) 300 °C, (◇) 350 °C, (+) 400 °C, (■) 450 °C, (□) 500 °C.

Table 5
Coulombic efficiencies (%) of surface-fluorinated NG-25 graphite samples

Graphite sample	Cycle number									
	1	2	3	4	5	6	7	8	9	10
Original graphite	85.6	95.0	96.6	97.4	97.4	97.6	98.1	98.1	98.2	98.4
Fluorinated at 150 °C	86.0	94.9	96.4	97.0	97.5	97.5	97.8	98.1	98.4	98.5
Fluorinated at 200 °C	86.3	95.2	96.7	97.3	97.9	98.1	98.5	98.7	99.3	98.9
Fluorinated at 250 °C	86.4	95.6	96.5	97.6	98.1	98.5	98.6	98.6	98.1	99.1
Fluorinated at 300 °C	85.9	94.9	96.8	97.2	97.9	98.3	98.6	98.6	98.8	99.0
Fluorinated at 350 °C	83.9	94.4	96.0	96.8	97.6	98.0	98.7	98.9	99.1	98.8
Fluorinated at 400 °C	79.7	93.9	94.1	95.9	97.5	97.4	97.9	98.5	98.6	98.4
Fluorinated at 450 °C	74.1	90.9	93.5	95.5	97.0	97.2	97.5	98.1	98.4	98.3
Fluorinated at 500 °C	66.5	89.5	91.6	94.7	96.8	97.5	97.9	98.0	98.2	98.2

Table 6
Coulombic efficiencies (%) of surface-fluorinated NG-40 graphite samples

Graphite sample	Cycle number									
	1	2	3	4	5	6	7	8	9	10
Original graphite	85.1	93.4	95.4	96.2	96.7	97.5	97.8	98.0	98.3	98.8
Fluorinated at 150 °C	86.1	95.1	96.1	97.4	97.6	97.6	98.0	98.5	98.8	99.2
Fluorinated at 200 °C	85.9	94.6	95.6	96.9	98.0	98.2	98.5	98.9	99.1	99.0
Fluorinated at 250 °C	86.3	94.7	95.9	97.1	97.5	98.1	97.8	98.3	98.5	98.2
Fluorinated at 300 °C	85.5	94.5	96.0	97.6	97.4	97.9	98.4	98.1	98.5	98.5
Fluorinated at 350 °C	83.4	93.7	95.2	96.5	96.9	96.9	98.1	97.8	98.4	98.3
Fluorinated at 400 °C	71.1	92.5	94.7	96.8	97.0	97.1	97.5	97.7	98.2	98.2
Fluorinated at 450 °C	72.2	91.8	94.2	95.4	96.2	96.5	96.9	97.5	98.1	98.0
Fluorinated at 500 °C	65.1	88.1	92.4	94.8	95.5	96.1	97.0	97.4	97.7	97.8

intercalation and deintercalation of lithium ion into and from graphite irrespectively of the surface fluorination. The R value obtained from Raman spectra of untreated graphite (NG-7) increased from 0.083 to 0.16 by charge/discharge cycling [5]. This structural change would induce the enlargement of the surface area of original graphite, leading to the increase in the reaction rate. In case of surface-fluorinated samples, the additional reason would be mentioned. The charge/discharge cycling for surface-fluorinated samples further increased the surface disordering to the higher degree [5]. This suggests that slightly larger amounts of excess lithium can be stored in the surface mesopores after 1st cycle in addition to the increase in the reaction rate.

The Coulombic efficiencies are given in Tables 5 and 6. Original graphite samples have the high first Coulombic efficiencies of 85.6 and 85.1%. The same first Coulombic efficiencies are obtained for both 25 and 40 μm graphite samples fluorinated between 150 and 300 °C. It means that the irreversible capacities induced by surface fluorine are negligible for the samples fluorinated in this temperature range. However, the first Coulombic efficiencies are gradually diminished with increasing fluorination temperature from 350 to 500 °C. The Coulombic efficiencies are increased with cycling and approach 97–98% after several cycles for the samples fluorinated between 150 and 300 °C, though the samples fluorinated at the higher temperatures need more several cycles to reach the same values of Coulombic efficiency.

As shown in Figs. 8 and 9, all the surface-fluorinated graphite samples demonstrate the higher capacities than original graphites. Among them, the 25 μm graphite samples fluorinated at 150–400 °C and 40 μm graphite samples fluorinated at 150–300 °C even show the higher capacities than the theoretical value of graphite, 372 mAh g^{-1}. The data for pore volume distribution of graphite are changed by surface fluorination as shown in Figs. 4–6. Surface fluorination at high temperatures causes carbon–carbon bond breaking and yields the mesopores with limited diameters such as 1.5–2, 2–3, 3–4 nm and so on. Among them, the mesopores with diameter of 2–3 nm are majority in any case. The capacities exceeding the theoretical value may be due to excess lithium accumulated in the surface mesopores with such diameters. The similar change in the surface structures are observed in the case of light oxidation of carbon materials [1,3].

4. Conclusions

It has been demonstrated in this study that surface modification by elemental fluorine effectively improves the electrochemical characteristics of graphite. The fluorination

of graphite samples with average particle diameters of 25 and 40 μm is made at a high temperature ranging from 150 to 500 °C by a low pressure fluorine gas (3×10^4 Pa) for 2 min. The surface fluorination of graphite powder causes the enlargement of surface area by 64–77% and a large amount of mesopores with diameter of 2–3 nm. These surface structure changes give rise to the increase in the capacities of surface-fluorinated graphite samples. Their capacities are larger than those of original graphite samples and even the theoretical capacity of graphite (372 mAh g^{-1}). The increments of the capacities are ∼10 and ∼13% for 25 and 40 μm graphite samples, respectively. The first Coulombic efficiencies for the samples fluorinated between 150 and 300 °C are the same as those for original graphites. Surface fluorination, thus, induces no increase in the irreversible capacity if the fluorination is performed between 150 and 300 °C.

Acknowledgements

The present study was financially supported by Grant-in-Aid for Research for the Future Program (nanocarbon) of Japan Society for the Promotion of Science (JSPS). The fluorine gas and graphite samples used were supplied by the courtesy of Daikin Industries Ltd. and Japan Storage Battery Co. Ltd., respectively. The authors gratefully thank them for their kind supports.

References

[1] E. Peled, C. Menachem, D. Bar-Tow, A. Melman, J. Electrochem. Soc. 143 (1996) L4–L7.
[2] M. Hara, A. Satoh, N. Tamaki, T. Ohsaki, Tanso 165 (1994) 261–267.
[3] J.S. Xue, J.R. Dahn, J. Electrochem. Soc. 142 (1995) 3668–3677.
[4] T. Nakajima, K. Yanagida, Tanso 174 (1996) 195–200.
[5] T. Nakajima, M. Koh, R.N. Singh, M. Shimada, Electrochim. Acta 44 (1999) 2879–2888.
[6] T. Nakajima, V. Gupta, R.N. Singh, Y. Ohzawa, A. Tressaud, E. Durand, J. Power Sources, in press.
[7] T. Takamura, M. Kikuchi, Battery Tech. 7 (1995) 29–38.
[8] R. Takagi, T. Okubo, K. Sekine, T. Takamura, Denki Kagaku 65 (1997) 333–334.
[9] M. Yoshio, H. Wang, K. Fukuda, Y. Hara, Y. Adachi, J. Electrochem. Soc. 147 (2000) 1245–1250.
[10] T. Nakajima, N. Watanabe, Graphite Fluorides and Carbon–Fluorine Compounds, CRC Press, Boca Raton, 1991.
[11] T. Nakajima, Synthesis, Structure, and Physicochemical Properties of Fluorine–Graphite Intercalation Compounds, in: T. Nakajima (Ed.), Fluorine–Carbon and Fluoride–Carbon Materials: Chemistry, Physics and Applications, Marcel Dekker, New York, 1995, pp. 1–31.
[12] I. Palchan, M. Crespin, H. Estrade-Szwarckopf, B. Rousseau, Chem. Phys. Lett. 157 (1989) 321–327.
[13] A. Tressaud, C. Guimon, V. Gupta, F. Moguet, Mater. Sci. Eng. B30 (1995) 61–68.
[14] Y. Matsuo, T. Nakajima, Z. Anorg. Allg. Chem. 621 (1995) 1943–1950.
[15] F. Tuinstra, J.L. Koenig, J. Chem. Phys. 53 (1970) 1126–1130.
[16] D.S. Knight, W.B. White, J. Mater. Res. 4 (1989) 385–393.
[17] R. Fong, U. von Sacken, J.R. Dahn, J. Electrochem. Soc. 137 (1990) 2009–2013.